

Motor Imagery Recognition for Brain-Computer Interfaces Using Hilbert-Huang Transform and Effective Event-Related-Desynchronization Features

Ching-An Cheng¹, Han-Pang Huang^{1*}, and Yi-Hung Liu²

¹ Department of Mechanical Engineering, National Taiwan University, Taipei, Taiwan

² Department of Mechanical Engineering, Chung Yuan Christian University, Chungli, Taiwan

Tel: (02)33662700, Email: hanpang@ntu.edu.tw

Abstract

Motor imagery recognition has been considered an important topic in the brain-computer interface (BCI) community. Due to noises and artifacts in signals, how to gain satisfactory classification accuracy is still a critical issue. We propose in this paper a novel method to address this issue. The method consists of three steps. Firstly, EEG signals from different electrodes are transformed into Hilbert spectrums by Hilbert-Huang Transform (HHT). A set of features are then extracted from the spectrums by the proposed feature extraction method. The features can effectively represent the event-related-desynchronization (ERD) during motor imagery. Finally, two different classification schemes are employed to accomplish the task of Motor imagery recognition. Experiments on the BCI 2003 competition data set indicate that our method achieve better classification accuracy and higher mutual information (MI) than the winner of the BCI 2003 competition.

Keywords: motor imagery, brain-computer interface Hilbert-Huang transform, mutual information, event related desynchronization

1. Introduction

The Brain Computer Interface (BCI) is an interface technique between human and computer which can help severely motor-disabled patients to communicate and control the environment [6], [7]. Usually the EEG signals are preprocessed to improve performance. High-Pass Filter and Low-Pass Filter are used to eliminate the noise and artifacts (EOG or EMG). However, the artifacts and the desired EEG are usually in the same frequency range. Various feature extraction methods have been proposed, such as ICA and PCA, etc. However the results are not satisfactory due to the non-stationary characteristics of EEG and the limited knowledge to the brain function. Therefore, how to extract distinguishing features from EEG becomes critical for motor imagery recognition.

During the imaginary movement, the energy of mu wave (8~12Hz) varies [2] [9]. Ideally, the Event-Related Desynchronization (ERD) should be found significantly in the electrode C3 and C4. However in practice, the

ERD is not easy to detect due to low SNR, making the problem of motor imagery recognition intractable. Previously, the raw EEG data is transformed into frequency domain by methods like Fourier Transform [8] and Wavelet Transform. Recently, some researches used the Hilbert-Huang Transform (HHT) [1]. The Hilbert spectrum in HHT provides a better transient response than that of Fourier Transform and Wavelet Transform. However the question lies on whether a better transient resolution provides us a better view for imaginary movement detection. Hilbert spectrum is more discrete than the frequency spectrum of Fourier Transform and Wavelet Transform. On the other hand, the ERD effect is a macroscopic phenomenon to time, while Hilbert spectrum shows as a microscopic view. Thus some modification must be made to suit for the classification of imaginary movement when using HHT. In this paper, we devise a method based on HHT. This method can effectively detect the ERD during motor imagery, thereby improving the classification performance.

This paper is organized as follows. In Section 2, we first describe the EEG data set used in this work. Then the HHT and analysis on EEG are given in Section 3. Section 4 introduces our method in detail. Experimental results are presented in Section 5. Conclusions are drawn in Section 6.

2. Data Description

The data used in this work are those from the Graz BCI competition III, 2003 [4]. The data were from a normal subject, a 25 years old female, during a feedback session. The session consists of 7 runs with 40 trials each. Each trial is of 9 s, and is illustrated in the paradigm as Fig. 1. In the period of 0-2 s, the subject was asked to relax. At $t=2$ s, an acoustic stimulus indicates that a motor imaginary task is ready to start, and then the symbol “+” is displayed on the screen for 1 s. Next, an arrow (left or right) is displayed as a cue, which lasts for 6s ($t=3$ to $t=9$). During the feedback period, the subject was asked to imagine a right or left hand movement. During the 9s-length trial, the EEG signals, recorded from C3, Cz, and C4, where Cz is a reference, were collected with a sampling rate of 128 Hz and filtered between 0.5 and 30 Hz.

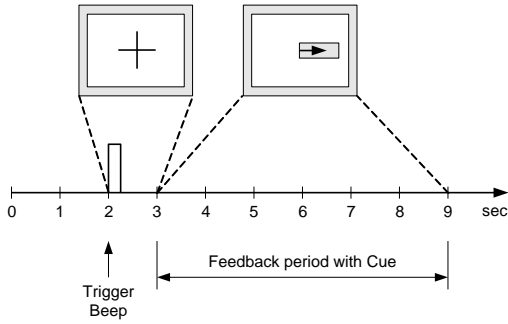


Fig.1 The paradigm of the Graz BCI competition III, 2003.

3. HHT and Analysis on EEG

The HHT consists of two parts: empirical mode decomposition (EMD), and Hilbert transform. First, the EMD decomposes an EEG signal $x(t)$ into intrinsic mode functions (IMFs) $c_j(t)$, $j=1, \dots, n$. The original signal can thus be expressed as

$$x(t) = \sum_{j=1}^n c_j(t) + r_n(t), \quad (1)$$

where $r_n(t)$ is the residue signal, which is a monotonic function and it stands for the mean trend of the original signal $x(t)$. In the EMD, the IMFs are generated by using a sifting process (please refer to [3] for more details on the sifting process), and the obtained IMFs will be almost adaptive, orthogonal, and complete.

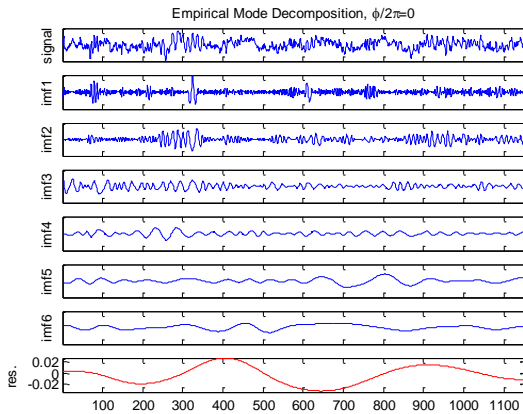


Fig. 2 EMD result on an EEG signal from C3 during one trial of 9 s. The left-hand imaginary movement was performed during 3-9 s.

Fig. 2 shows the EMD result on a 9s EEG signal from C3 during one trial, where the task of left-hand imaginary movement was performed within 3-9 s. The top subfigure shows the original EEG signal. Note that only six IMFs were extracted and shown in Fig. 2 because the remaining IMFs are close to useless: they have almost no contribution to the detection of ERD. Namely, the bottom signal is not the real residue since it is not monotonic. It can be observed from Fig. 2 that the first two IMFs have higher frequency components than the other four.

After performing the EMD on $x(t)$, we obtain a set of IMFs. The Hilbert transform is then performed on each IMF $c_j(t)$ to compute its Hilbert spectrum,

$$y_j(t) = \frac{PV}{\pi} \int_{-\infty}^{\infty} \frac{c_j(\tau)}{t-\tau} d\tau, \quad (2)$$

where PV denotes the Cauchy principal value. With the Hilbert spectrum, the analytic signal $z_j(t)$ is defined as the following complex series,

$$z_j(t) = c_j(t) + iy_j(t) = a_j(t)e^{i\theta_j(t)}, \quad (3)$$

where $a_j(t) = \sqrt{c_j(t)^2 + y_j(t)^2}$ is the instantaneous amplitude of $c_j(t)$, and $\theta_j(t) = \tan^{-1}(y_j/c_j)$ is the phase function. Finally, the instantaneous frequency

$$\omega_j(t) = \frac{d\theta_j(t)}{dt} \quad (4)$$

can be obtained. The advantage of the Hilbert transform over the fast Fourier transform (FFT) is clear: Hilbert spectrum can represent the time-frequency-magnitude variations, whereas the FFT spectrum can present only frequency-magnitude variations. Fig. 3 shows the Hilbert spectrums of the IMFs from the C3 and C4 EEG during left-hand imaginary movement, respectively. It can be observed from Fig. 3 that in 3-9 s, the alpha-band energy of C3 is relatively higher, which indicates that the C4 Hilbert spectrum can effectively reflect the ERD result during left-hand motor imagery.

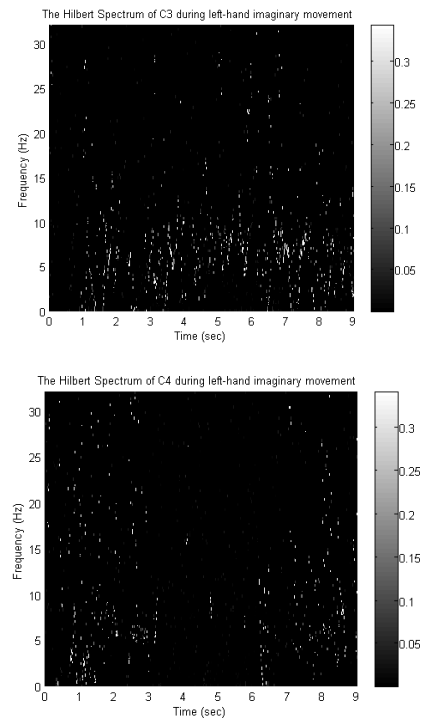


Fig. 3. The Hilbert spectrums of C3 (top) and C4 (bottom).

4. Method

4.1 Choice of IMFs

While HHT appears to be effective in detecting ERD, it is computationally expensive. A large number of iterations will be required in generating each IMF, making the EMD process time-consuming. As defined, the EMD process is stopped until a monotonic function (the residue) is obtained. However, one does not need to accomplish the whole EMD process in practice. In other words, even if all IMFs of an EEG signal are found, not all of them will be useful for the detection of ERD. Fig. 4 summarizes the energy contribution of the IMFs shown in Fig. 2. The sum of the energy of the first three IMFs contributes more than 80% of the total energy of the raw EEG signal, and the other part of the energy is almost equally distributed over the rest.

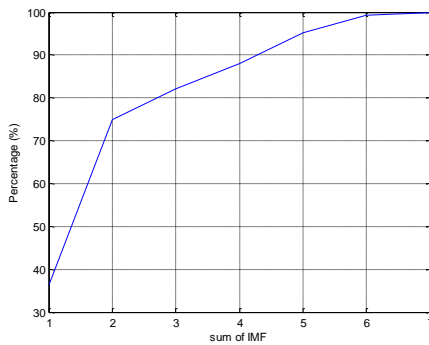


Fig. 4. The contribution of different IMFs of EEG signals. The label 1 in the x axis denotes the first IMF, and label 2 denotes the percentage of the energy contributed by the 1st and the 2nd IMFs and so on.

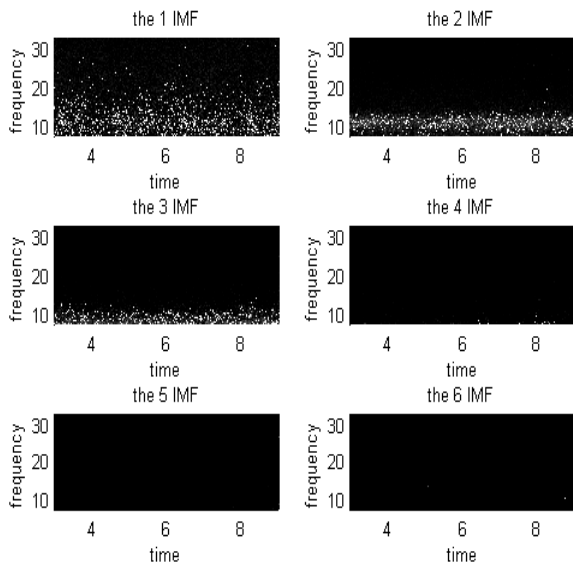


Fig. 5. The top left figure shows the averaged Hilbert spectrum of the first IMFs of the 140 EEG signals recorded from 140 trials of motor imagery, and so on. The frequency range of each IMF is different from each other.

Fig. 5 gives another view of how different IMFs take part in an EEG signal. Fig. 5 is the averaged Hilbert spectrum of 140 different EEG signals of imaginary movement, where the numbers of right-hand and left-hand imaginary movements are equal. It shows that the first IMF stochastically well distributed over the frequency range from DC to 32Hz, the second IMF focuses on the frequency range from 8 to 13Hz, the third IMF occupies the frequency range from DC to 10Hz, and the frequency ranges of the other IMFs mainly lie near DC. It follows that the first three IMFs have already enough information needed for ERD detection. Therefore, in this work each EEG signal is decomposed six IMFs by EMD, and the first three of them are used to generate the Hilbert spectrum. Next, we introduce how to extract features from the Hilbert spectrum.

4.2 Feature Extraction on the Hilbert spectrum

Our method extracts features from a moving window over the Hilbert spectrum. For a time point t , its corresponding moving window is within the interval of $[t, t + \Delta t]$, where Δt is the size of the window. As mentioned, the ERD occurs on the contralateral side of the brain when performing a right-hand or left-hand motor imagery task. We therefore propose a new feature extraction method which can effectively represent the energy difference in alpha band between the signals from channels C3 and C4.

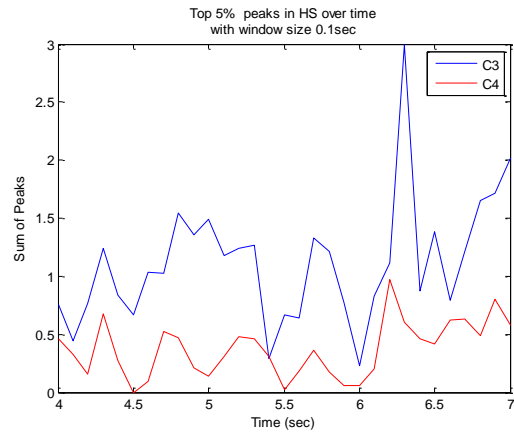


Fig. 6. The sum of top energy peaks (STEP) in the Hilbert spectrum (HS) over time as a feature during the left-hand imaginary movement.

However, different from the conventional methods which consider the total energy in the alpha band, our method considers only the sum of some highest time-frequency components in the alpha band. For example, on the Hilbert spectrum, if there are m time-frequency components falling into the alpha band within the moving window, we do not consider all of them but select some components which have higher energy. Note that the number m is determined by the window size Δt . Hence, only top $p\%$ energy peaks, i.e., top m' energy peaks where $m' = m \times p\%$, will be

chosen. By doing so, the noises will be eliminated for their energy is relatively lower. At each time point, the *sum of top energy peaks* ($STEP(t)$) is calculated as a feature for each channel. With the feature STEP, ERD during left-hand imaginary movement can be easily detected, as indicated in Fig. 6, where the STEP of C3 is significantly larger than that of C4 at all time points, except for the time point $t = 5.4s$. Based on the feature STEP, we further devise two kinds of classification schemes for comparison.

4.3 Classification Schemes

● Classification Scheme I

To facilitate the following description, we first define two terminologies. (1) *Starting time* t_s : it is the time point that the classification task starts. For BCI 2003 competition data set, $t_s \geq 3$ because the motor imagery tasks were performed at $t = 3s$. (2) *Classification time interval* (CTI): it denotes the interval from t_s to the time point that the classification task ends. Clearly, for BCI 2003 competition data set, $CTI \leq 6s$ because all the motor imagery tasks lasted for 6s. Moreover, the CTI should be much longer than the window size Δt .

Suppose that there are k time points within the classification time interval. Clearly, $k = CTI / \Delta t$. Our scheme compares the STEPs between C3 and C4 each of the k time points. For a time point, if the STEP of C3 is larger than that of C4, the time point is classified as left-hand imaginary movement (positive); right-hand imaginary movement (negative) otherwise. After the k time points are classified, we get k results. Then, the final classification is determined by using majority voting strategy: if the number of positive results is larger than that of negative results, we say that the EEG signals of C3 and C4 within the classification time interval belongs to the left-hand imaginary movement; right-hand imaginary movement otherwise. Moreover, if the true class label for this time interval is positive, i.e., the EEG signals within this time interval were actually recorded from a left-hand imaginary movement, we say that the classification result on this time interval is correct; otherwise it is a classification error. Therefore, for a specific classification time interval, an average classification rate is obtained since the BCI 2003 competition data set contains 140-trial signals.

In addition to the number of top energy peaks (i.e., the percentage of the energy peaks selected p) and size of the moving window Δt , the starting time t_s and the CTI are also free parameters, provided that in the 9s EEG, when the classification starts and how long it lasts affect largely the classification accuracy and MI [4][5]. The goal is to obtain the best starting time point with the shortest classification time interval.

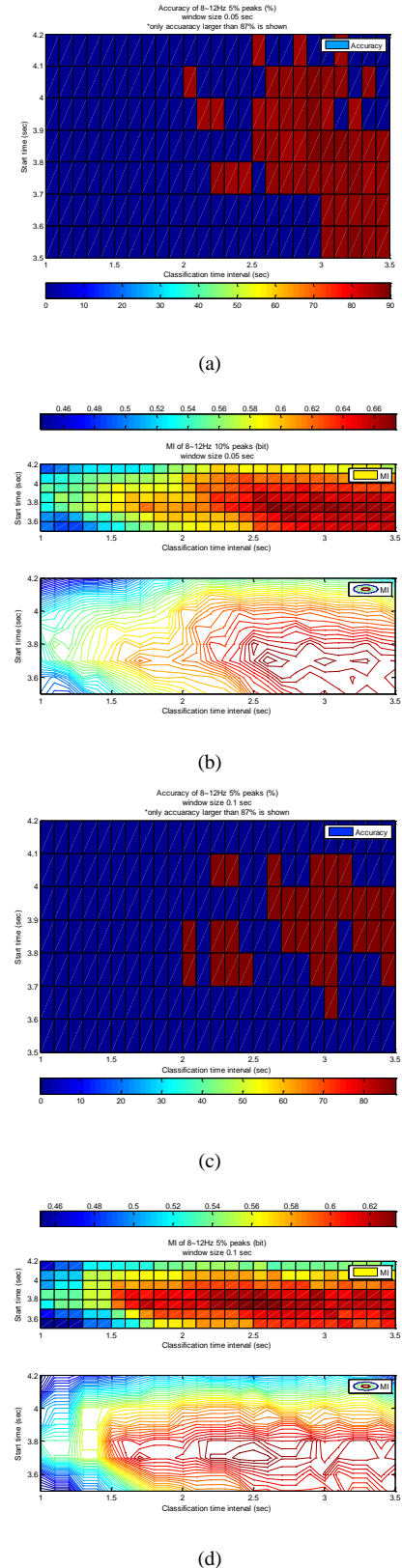


Fig. 7. The classification accuracy ((a) and (c)) and MI ((b) and (d)) obtained from scheme I. In the accuracy plots, the points with accuracy higher than 87% are marked red and the others are mared blue. The window sizes in (a) and (b) are 0.05 s, while in (c) and (d) the window sizes are set as 0.1 s. When extracting the feature STEP at each time point, the top 5% energy peaks were chosen.

Fig. 7 shows the results of classification accuracy and MI with different parameter combinations. As shown in Fig. 7, different combinations of t_s and CTI result in different classification accuracy and MI. The best CTI can be obtained by choosing the CTI with the highest MI.

● Classification Scheme II

In scheme II, the only difference is that the areas under surrogate signals are considered not the amplitudes. This scheme is physically an alternative opinion how ERD occurs. Unlike the first scheme the information of the past is considered, which makes this algorithm a casual MA model.

The second scheme gains a prospect of ERD. In Fig. 8 (the same trial as in Fig. 6), the area under the surrogate signals increases with time, which is a function of time $s(t)$. Thus two features can be obtained in this scheme. The first feature is how the area $s(t)$ varies with time. For each time point, the magnitude of two $s(t)$ (C3, C4) is compared, if $s(t)$ of C3 is larger than it's classified as left side imaginary movement, and vice versa. The second feature is the total area under the surrogate signal during a specific time interval, which is the final value of $s(t)$. This feature can be interpreted as the total effective energy difference during the time. If the final value of C3 is higher, then it is classified as left-side imaginary movement, and vice versa.

In practice, this scheme performs in a cumulative manner. The optimized classification time interval is calculated in the similar way as the first scheme to obtain the best performance, and a tradeoff between time delay and MI should also be made.

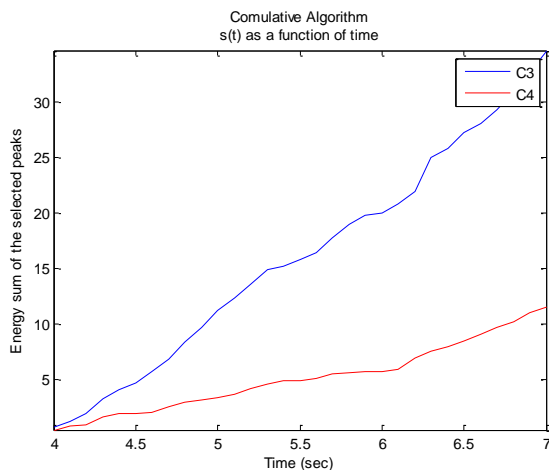


Fig. 8. This figure represents how the area under the two surrogates varies with time. Two features are gained with this figure. First, the amplitude of each time instants can be compared. Second, the final value, i.e. the total area, can be compared.

5. Experimental Results

The two classification schemes are tested with the test

data provided by Graz in order to compare with the results of the competition. Table 1 lists the results of the two classification schemes with optimized CTI obtained by the MI tables, and Table 2 shows the top 4 results of the Graz BCI competition 2003. The first column in Table 1 is described as follows.

- A is the first scheme with window size 0.05 s, top 10% peaks, and classification time interval 2.6 s.
- B is the first scheme with window size 0.05 s, top 10% peaks, classification time interval 1.7 s.
- C is the second scheme with window size 0.05s, top 10% peaks, and classification time interval 3.7 s. The first feature is used.
- D is the second scheme with window size 0.05s, top 10% peaks, and classification time interval 2.6 s. The second feature is used.
- E is the second scheme with window size 0.05s, top 10% peaks, and classification time interval 1.1 s. The second feature is used.

Table 1. The results of the proposed method using HHT.

Method	Min Error (%)	Max MI (bit)	Time (s)
A	11.43	0.63	6.4
B	13.57	0.58	5.6
C	12.14	0.69	7.5
D	10.71	0.68	6.4
E	17.86	0.48	5.1

Table 2. The top 4 results of the BCI competition 2003 [4].

Ranking	Min Error (%)	Max MI (bit)	Time (s)
1	10.71	0.61	7.59
2	15.71	0.46	5.05
3	17.14	0.45	6.70
4	13.57	0.44	4.18

It is noticed that all the methods in Table 1 are our proposed method. The optimal classification time intervals (CTIs) of A, C and D are determined according to the MI table of the training data. The CTIs of B and E are arbitrarily chosen. Namely, the CTIs for B and E are not optimum actually: they were chosen for comparison. Though both B and E have lower maximum MIs than A, C and D, they still perform better than the second ranking of the BCI 2003 competition in terms of MI. Moreover, according to Table 1, the best method is D, which has high MI and the smallest classification error rate. Also, its minimum error is the same as the first ranking (i.e., the winner) of the competition; however, its MI is much higher and its time delay is shorter.

To further compare method D with the top 4 winners

of the competition, Fig. 9(a) shows the variation of MI of D with different time instants, and Fig. 9(b) shows the results of the competition. The top four winners of the competition in Table 2 are C, F, B, and A in Fig. 9(b), respectively. As can be seen from Fig. 10, our method (method D) outperforms all the winners of the BCI 2003 competition. The effectiveness of the proposed method in improving the performance of motor imagery recognition has been demonstrated.

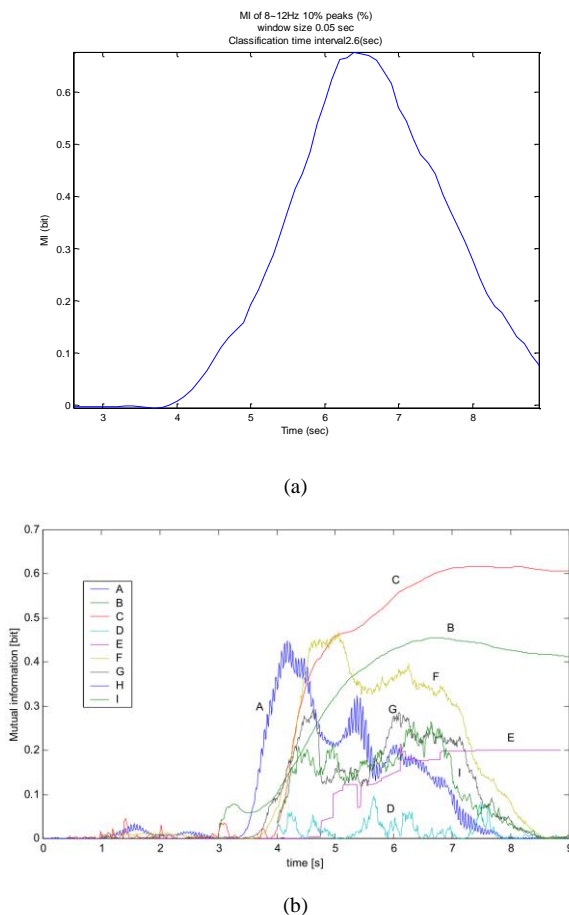


Fig. 9. Comparison of the mutual information between (a) our method and (b) the winners of BCI 2003 competition.

6. Conclusion

In this paper, we have presented a novel method to improve the performance of motor imagery recognition. The results carried out on the EEG data provided by the BCI 2003 competition has indicated the effectiveness of the proposed method. Compared with the winner of the competition, our method achieves higher mutual information and shorter time delay. The success of our method should be attributed to the use of HHT and a robust feature extraction method, which is capable of extracting discriminating features from the Hilbert spectrum such that the ERD is effectively detected.

During the imaginary movement it's impossible to ensure that he subject is really performing the right imagination. In the Hilbert Spectrums of the subjects,

we can observe that ERD does not occur all the time, and the mostly during 3.8 to 6 sec. Thus when using this method in real online BCI, some consideration must be made. The classification algorithm for this paradigm is suited for a clock-like BCI. For example, the EEG signal is scanned each 6 seconds and the result presents the decision of the time period. However a 6-second interval is too long for online BCI, a shorter period paradigm has to be made to obtain the optimized parameters for an online BCI using these algorithms.

In the presented method, the classification strategy is quite simple. In the future, we will involve more sophisticated classifiers, such as support vector machines (SVMs), for comparison.

References

1. Norden E. Huang, Zheng Shen, Steven R. Long et al., *The empirical mode decomposition and the Hilbert spectrum for nonlinear and non-stationary time series analysis*, 1996.
2. J. A. Pineda, "The functional significance of mu rhythms: translating "seeing" and "hearing" into "doing"", *Brain Research Reviews*, Vol. 50, no. 1, 1 pp. 57-68, Dec. 2005,
3. Gabriel Rilling, Patrick Flandrin et al., "On Empirical Mode Decomposition and Its Algorithm,
4. A. Schlögl. "Outcome of the BCI-competition 2003 on the Graz data set," http://www.bbc.de/competition/ii/results/TR_BCI2_003_III.pdf.
5. Alois Schlögl, *The Electroencephalogram and the Adaptive Autoregressive Model: Theory and Applications*, 2000
6. Hong-Gi Yeom, Kwee-Bo Sim, "ERS and ERD Analysis during the Imaginary Movement of Arms", *International Conference on Control, Automation and Systems*, 2008
7. J. R. Wolpaw, N. Birbaumer, D. J. McFarland et al., "Brain-computer interfaces for communication and control," *Clinical Neurophysiology*, vol. 113, no. 6, pp. 767-791, 2002.
8. P. G. Pregoner M, "Frequency component selection for and EEG-based brain computer interface.," *IEEE Trans. Rehabil. Eng.*, vol. 7, pp. 413-419, 1999.
9. G. Pfurtscheller, "Graphical display and statistical evaluation of desynchronization (ERD)," *Electroencephalography and Clinical Neurophysiology*, vol. 43, no. 5, pp. 757-760, 1977.
10. D. J. McFarland, L. A. Miner, T. M. Vaughan et al., "Mu and beta rhythm topographies during motor imagery and actual movements," *Brain Topography*, vol. 12, no. 3, pp. 177-186, 2000.